Journal of the American Heart Association

ORIGINAL RESEARCH

Increased Myocardial Oxygen Consumption Precedes Contractile Dysfunction in Hypertrophic Cardiomyopathy Caused by Pathogenic *TNNT2* Gene Variants

Rahana Y. Parbhudayal, MD; Hendrik J. Harms, PhD; Michelle Michels, MD, PhD; Albert C. van Rossum, MD, PhD; Tjeerd Germans, MD, PhD; Jolanda van der Velden, PhD

BACKGROUND: Hypertrophic cardiomyopathy is caused by pathogenic sarcomere gene variants. Individuals with a thin-filament variant present with milder hypertrophy than carriers of thick-filament variants, although prognosis is poorer. Herein, we defined if decreased energetic status of the heart is an early pathomechanism in *TNNT2* (troponin T gene) variant carriers.

METHODS AND RESULTS: Fourteen individuals with *TNNT2* variants (genotype positive), without left ventricular hypertrophy (G+/LVH−; n=6) and with LVH (G+/LVH+; n=8) and 14 healthy controls were included. All participants underwent cardiac magnetic resonance and [^{11}C]-acetate positron emission tomography imaging to assess LV myocardial oxygen consumption, contractile parameters and myocardial external efficiency. Cardiac efficiency was significantly reduced compared with controls in G+/LVH− and G+/LVH+. Lower myocardial external efficiency in G+/LVH− is explained by higher global and regional oxygen consumption compared with controls without changes in contractile parameters. Reduced myocardial external efficiency in G+/LVH+ is explained by the increase in LV mass and higher oxygen consumption. Septal oxygen consumption was significantly lower in G+/LVH+ compared with G+/LVH−. Although LV ejection fraction was higher in G+/LVH+, both systolic and diastolic strain parameters were lower compared with controls, which was most evident in the hypertrophied septal wall.

CONCLUSIONS: Using cardiac magnetic resonance and [^{11}C]-acetate positron emission tomography imaging, we show that G+/LVH− have an initial increase in oxygen consumption preceding contractile dysfunction and cardiac hypertrophy, followed by a decline in oxygen consumption in G+/LVH+. This suggests that high oxygen consumption and reduced myocardial external efficiency characterize the early gene variant–mediated disease mechanisms that may be used for early diagnosis and development of preventive treatments.

Key Words: cardiac efficiency ■ hypertrophic cardiomyopathy ■ oxygen consumption ■ *TNNT2*

Hypertrophic cardiomyopathy (HCM) is the most common inherited cardiac disease and occurs with an estimated prevalence of 1:200 in the general population.[1] HCM is characterized by isolated left ventricular hypertrophy (LVH), which cannot be explained by abnormal loading conditions.[2] In ≈50% to 60% of all cases, a sarcomere gene variant is identified.[3] Although most variants are present in genes encoding thick-filament proteins of the sarcomere, a subset of patients with HCM have thin-filament gene variants.[4] The most frequently affected thin-filament gene, *TNNT2* (troponin T gene), encoding cardiac troponin T,[5] accounts for 2% to 5% of all HCM cases.[6]

Patients with HCM harboring *TNNT2* gene variants present with a relatively mild form of hypertrophy compared with patients with thick-filament gene variants,

Correspondence to: Jolanda van der Velden, PhD, Department of Physiology, Amsterdam University Medical Center, Vrije Universiteit Amsterdam, De Boelelaan 1117, 1081 HV Amsterdam, The Netherlands. E-mail: j.vandervelden1@amsterdamumc.nl

Supplementary Material for this article is available at https://www.ahajournals.org/doi/suppl/10.1161/JAHA.119.015316

For Sources of Funding and Disclosures, see page 11.

JAHA is available at: www.ahajournals.org/journal/jaha

CLINICAL PERSPECTIVE

What Is New?

- This study shows reduced cardiac efficiency at preclinical and hypertrophic cardiomyopathy disease stage in individuals carrying a *TNNT2* (troponin T gene) variant.
- At a regional level, analysis showed significantly higher myocardial oxygen consumption in the septal and lateral left ventricular wall of gene variant carriers without left ventricular hypertrophy and the lateral wall of gene variant carriers with left ventricular hypertrophy compared with controls, indicating that the presence of a *TNNT2* gene variant increases local oxygen consumption and reduces efficiency of cardiac contraction.

What Are the Clinical Implications?

- This study shows that the increase in myocardial oxygen consumption in *TNNT2* gene variant carriers precedes changes in global and regional myocardial contractility, indicating that the energetic status rather than contractile parameters reflects the initial variant-induced pathomechanism that can be used for early diagnosis and preventive therapy.

Nonstandard Abbreviations and Acronyms

BSA	body surface area
CMR	cardiac magnetic resonance
EW	external work
G+/LVH+	genotype positive/left ventricular hypertrophy positive
G+/LVH–	genotype positive/left ventricular hypertrophy negative
HCM	hypertrophic cardiomyopathy
LGE	late gadolinium enhancement
LV	left ventricle
LVM	left ventricular mass
MEE	myocardial external efficiency
MVO_2	myocardial oxygen consumption
MYBPC3	myosin-binding protein C gene
MYH7	β-myosin heavy chain gene
PET	[^{11}C]-acetate positron emission tomography
SCS	systolic circumferential strain
TNNT2	troponin T gene

while they have a poorer prognosis.[5,7–9] A study by Coppini and colleagues showed that individuals with thin-filament variants are characterized by more adverse remodeling and more severe diastolic dysfunction compared with patients with thick-filament gene variants.[5] Another HCM patient cohort study showed that thin-filament gene variant carriers had a greater probability of heart failure–related death than individuals carrying thick-filament gene variants.[9] Studies in HCM rodent models and human cardiac tissue have consistently shown that myofilaments with *TNNT2* gene variants are characterized by an increased myofilament Ca^{2+} sensitivity, perturbed length-dependent myofilament activation, and increased cross-bridge kinetics and energetics.[10–13] To understand how these *TNNT2* gene variant–mediated myofilament changes translate to changes in cardiac phenotype, a better understanding of the cardiac changes at preclinical and HCM disease stage is warranted.

Noninvasive imaging studies have demonstrated impaired cardiac energetics in both animals and humans with HCM,[14–16] and even in carriers (genotype positive) without hypertrophy (G+/LVH).[17] Individuals with thick-filament gene variants showed reduced myocardial efficiency compared with healthy controls.[18] In addition, carriers harboring *MYH7* (β-myosin heavy chain gene) variants demonstrated a more prominent reduction of myocardial efficiency compared with *MYBPC3* (myosin-binding protein C gene) carriers, indicative for a gene-specific effect.[19] Moreover, myocardial efficiency was further decreased in patients with obstructive HCM at the time of myectomy.[19]

As energetic alterations may play an important role in the preclinical stage of HCM pathophysiological characteristics, and may serve as a target for future therapy,[13,14,20] herein we investigated if myocardial efficiency is altered at preclinical (genotype positive/LVH negative [G+/LVH–]) and HCM disease stage (genotype positive/LVH positive [G+/LVH+]) in *TNNT2* gene variant carriers. Myocardial external efficiency (MEE) (ie the ratio between external work [EW]/myocardial oxygen consumption [MVO_2]), was assessed in vivo by state-of-the-art [^{11}C]-acetate positron emission tomography (PET) and cardiac magnetic resonance (CMR) imaging in 6 G+/LVH– and 8 G+/LVH+ individuals.

METHODS

The data that support the findings of this study are available from the corresponding author on reasonable request.

Study Population

The study was approved by the local Ethics Committee and was performed in agreement with the Declaration of Helsinki. All participants gave written informed consent before inclusion. All preclinical gene variant carriers (G+/LVH–; n=6) and genotype-positive HCM (G+/

LVH+; n=8) patients were prospectively enrolled between March 2017 and October 2018. All participants were genetically tested positive for variants in the *TNNT2* gene. Classification into the G+/LVH– and G+/LVH+ groups was based on the criteria for septal thickness, as proposed in the current European Society of Cardiology guidelines (ie, HCM is defined by a wall thickness ≥15 mm [≥13 mm in case of first-degree family members] in ≥1 LV myocardial segments in the absence of any other cardiac or systemic condition likely to cause LV hypertrophy). In addition, maximal wall thickness for the G+/LVH– group was set at ≤10 mm. Exclusion criteria were septal reduction therapy or heart transplantation in their medical history, renal impairment (<30 mL·min^{-1}·1.73 m^{-2}), hypertension, and any relative or absolute contraindication to undergo a CMR scan. Fourteen healthy individuals served as the control group (data of the control group have been published before).[19] Before the imaging protocols, from all participants, blood samples were drawn and NT-proBNP (N-terminal pro-B-type natriuretic peptide; expressed in ng·L^{-1}), hemoglobin, creatinine, glucose, free fatty acid, and lactate levels were determined.

Cardiac Imaging Studies

Transthoracic echocardiography

To derive LV outflow tract gradients and diastolic function, continuous-wave Doppler was applied, according to the American Society of Echocardiography guidelines.[21] Septal diastolic mitral annular velocity and peak early diastolic mitral inflow velocity were measured in the apical 4-chamber view.

CMR and positron emission tomography imaging

All participants underwent CMR imaging on a 1.5-T whole body scanner (Avanto; Siemens, Erlangen, Germany), using a 6-channel phased-array body coil. Cine images were obtained using a standard retrospective gated, single breath-hold segmented k-space balanced steady-state free sequence, with contiguous short axis slices to cover the whole LV from base to apex.

PET was performed to noninvasively assess oxygen metabolism using the rate constant K_2, which represents the rate of transfer of radioactivity from tissue to blood from which MVO_2 is derived.[22] All participants underwent a PET scan, after overnight fasting, on a Gemini TF-64 PET/CT scanner (Philips Healthcare, Best, The Netherlands). Data of the control group were acquired as described previously.[23] Representative CMR and PET images are depicted in Figure 1. Reproducibility of CMR/PET analysis was high, with low intraobserver and interobserver variability.[18] For additional image acquisitions on CMR and PET, see Data S1.

Post processing

The CMR cine images were analyzed off-line using MASS analysis software, version 2.1 (Medis Medical Imaging Systems, Leiden, The Netherlands). End-diastolic and end-systolic volumes of the LV and LV ejection fraction were obtained by application of the endocardial contours. Addition of epicardial contours resulted in LV mass (LVM). End-diastolic wall thickness at the septum was derived from the mean of 4 septal segments (anteroseptal and inferoseptal) at the basal and midventricular level. Tissue tagging images were analyzed by inTag (https://www.creatis.insa-lyon.fr/osirix-dev/CardiacTools.html) software (CREATIS, Lyon, France) to quantify myocardial deformation using the SinMod technique and estimate regional peak circumferential strain components (systolic circumferential strain [SCS] and diastolic circumferential strain rate). Myocardial strain was measured in the midmyocardial layer, which has been reported to be the most reproducible.[24] The software runs as a plug-in for OsiriX, version 6.5 (Pixmeo, Switzerland).[25] Analysis of the LV was calculated according to the 17-segment American Heart Association model.[26] Late gadolinium enhancement (LGE) was assessed by applying the full width at half maximum method on the LGE cine short axis images and is expressed as percentages of the LV mass.[27] The aQuant software package was used for analysis of dynamic PET data.[28] The product of stroke volume and mean arterial pressure, which yield EW, and PET-derived MVO_2 allows assessment of MEE, according to the following equation:

$$\mathrm{MEE} = \frac{\mathrm{EW} \cdot \mathrm{HR} \cdot 1.33 \cdot 10^{-4}}{\mathrm{MVO_2} \cdot \mathrm{LVM} \cdot 20}$$

HR represents the heart rate, and the caloric equivalent of 1 mm Hg·mL EW is 1.33·10^{-4}, whereas 1 mL O_2 corresponds to 20 J.[29]

As hypertrophy in HCM is asymmetric, affecting the septum of the heart, changes in myocardial function and efficiency may differ between LV regions. Efficiency was therefore determined in the septum and lateral wall of the LV as the ratio between regional SCS and the corresponding $MVO_{2(beat)}$ according to the 17-segment model of the American Heart Association.[26] Less negative values indicate reduced efficiency.[19]

Statistical Analysis

Statistical analysis was performed using SPSS software, version 22.0 (SPSS, Chicago, IL). Normality of data was inspected visually by means of QQ-plots.

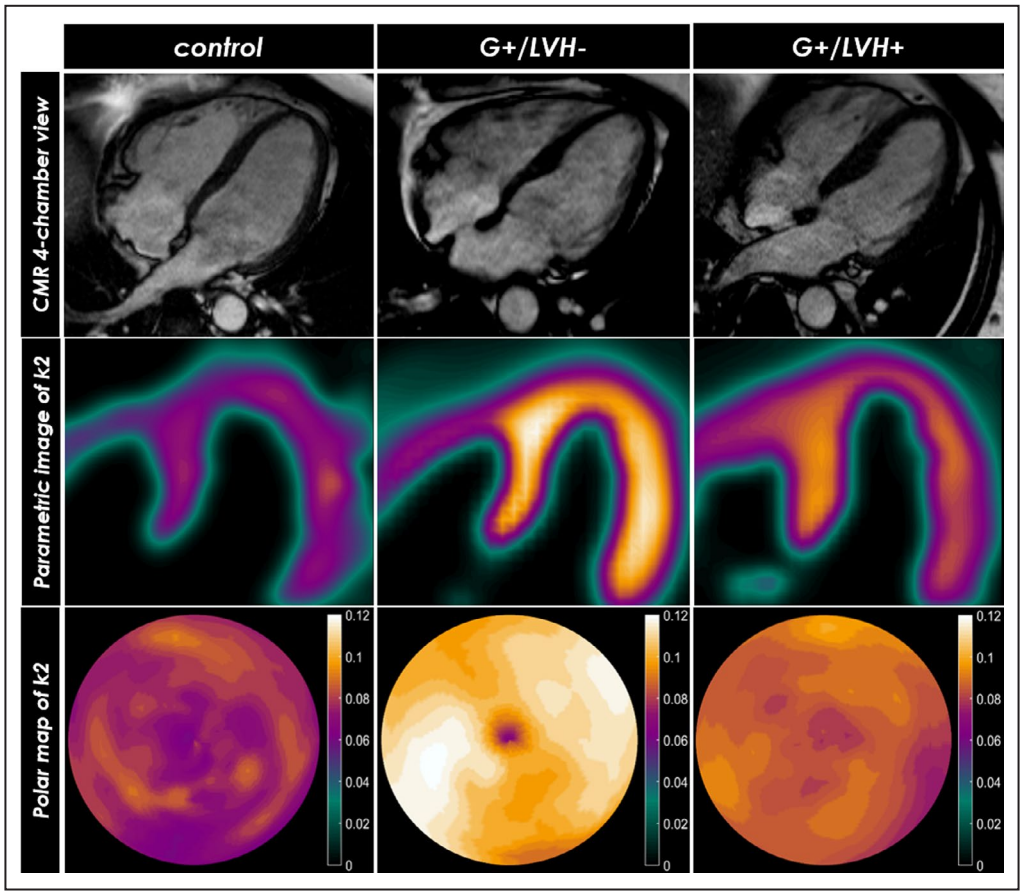

Figure 1. Cardiac images of control, genotype-positive/left ventricular hypertrophy–negative (G+/LVH–), and genotype-positive/left ventricular hypertrophy–positive (G+/LVH+) individuals. Examples of a cardiac magnetic resonance (CMR) 4-chamber view and parametric images of [^{11}C]-acetate positron emission tomography–derived images and the corresponding polar maps are shown for control, G+/LVH–, and G+/LVH+. k2 indicates average [^{11}C]-acetate clearance rate constant.

The χ^2 test was used for categorical demographic variables. Means of continuous variables were compared between groups using ANOVA tests after normality was verified or a Mann-Whitney *U* test if data were not normally distributed. In case of a significant overall ANOVA test, post hoc tests were performed with a Bonferroni correction to account for multiple comparisons. An (overall) 2-sided significance level of 5% was used for all statistical tests.

RESULTS

Recruitment and Characteristics of Controls, G+/LVH–, and G+/LVH+

Participants were recruited from clinical centers in The Netherlands, including Amsterdam University Medical Center, Leiden University Medical Center, and Erasmus Medical Center. In total, 85 individuals were identified with a pathogenic *TNNT2* gene variant (Figure 2). Four (5%) eligible G+/LVH– individuals and 6 (7%) eligible G+/LVH+ were included. The remaining subjects were excluded because of the following reasons: 22 (26%) were aged >65 years, 18 (21%) could not be reached, 12 (14%) had an implantable cardioverter-defibrillator, 10 (12%) had cardiac phenotypes other than HCM, 5 (6%) refused participation for different reasons, and the remaining group consisting of 8 patients (9%) had died in the past years, had atrial fibrillation, had type 2 diabetes mellitus, carried a gene variant of unknown significance, and/or had a LV wall thickness measuring between 10 and 15 mm. In both G+/LVH– and G+/LVH+ groups, 2 subjects were included via their family member. The G+/LVH– group includes one identical twin. Because of the difficulty to include eligible G+/LVH–, this group consisted only of women. Analysis of MVO_2 and MEE in our control group did not show sex differences (Table S1), indicating that sex does not introduce a bias. *TNNT2* variants of G+/LVH– and G+/LVH+ are listed in Table 1 and shown in the schematic figure of the thin filament in Figure 3.[30] G+/LVH– and controls did not use medication. G+/LVH+ had a lower

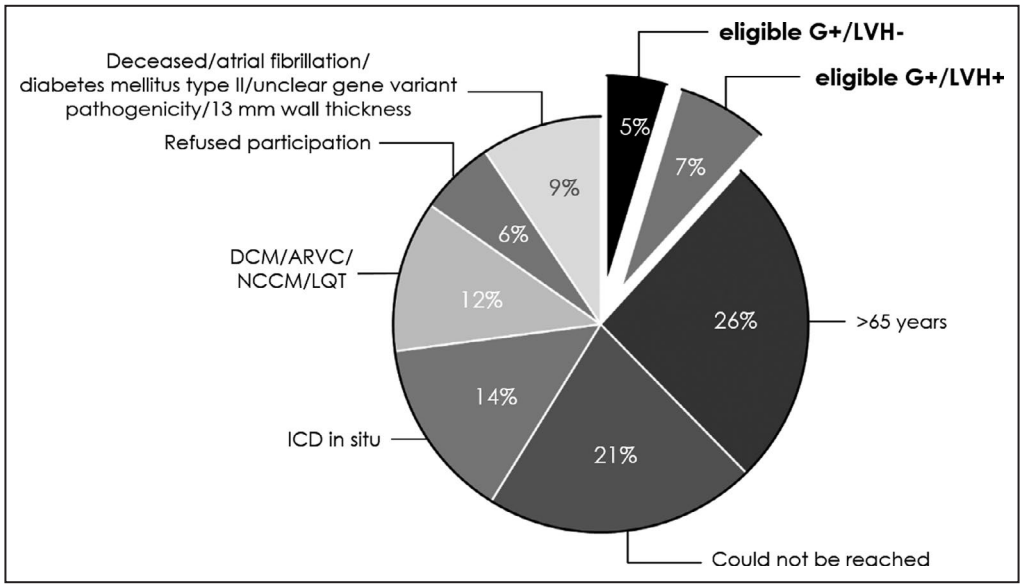

Figure 2. Distribution of *TNNT2* (troponin T gene) variant-positive individuals.
In total, 85 individuals were identified with a pathogenic *TNNT2* gene variant. Among these, 5% eligible genotype positive/left ventricular hypertrophy negative (G+/LVH–) and 7% eligible genotype positive/left ventricular hypertrophy positive (G+/LVH+) were included. The remaining individuals were excluded because of the reasons indicated in each slice. ARVC indicates arrhythmogenic right ventricular cardiomyopathy; DCM, dilated cardiomyopathy; ICD, implantable cardioverter-defibrillator; LQT, long-QT syndrome; and NCCM, noncompaction cardiomyopathy.

heart rate compared with controls (Table 1, Figure 4), most likely explained by the use of β blockers in this group. Systolic and diastolic blood pressures were comparable between all groups. Individuals in the G+/LVH+ were predominantly men and showed elevated levels of NT-proBNP (Table 1).

G+/LVH+ had a significantly higher maximal septal and lateral wall thickness than G+/LVH– and controls (Table 1), although no obstruction was evident from low LV outflow tract gradients (Table 1). In accordance with a higher wall thickness in G+/LVH+, LV mass in G+/LVH+ was higher compared with G+/LVH– and controls (Table 1, Figure 4). LV end-diastolic volume and stroke volume were lower in G+/LVH– compared with controls, which is explained by female predominance in the G+/LVH– group (Table 1).[31] G+/LVH+ and controls had comparable LV end-diastolic volume and stroke volume (Table 1). None of the G+/LVH– subjects and controls had contrast enhancement on LGE images. Of 8 G+/LVH+ subjects, 7 had contrast enhancement on LGE imaging, which indicates fibrosis, with a median estimated percentage of 7%, mainly located at the right ventricle insertion points. LV ejection fraction was significantly higher in G+/LVH+ compared with controls, whereas global peak circumferential strain in G+/LVH+ was significantly lower compared with G+/LVH– and controls (Tables 1 and 2). LV ejection fraction and global peak circumferential strain in G+/LVH– were similar to controls (Tables 1 and 2).

With respect to regional function, septal peak SCS in G+/LVH+ was significantly lower than G+/LVH– and controls, whereas lateral peak SCS was similar as in G+/LVH– and controls (Table 2). Septal and lateral peak SCS in G+/LVH– were similar as in controls (Table 2). Septal peak diastolic circumferential strain rate was significantly lower in G+/LVH+ compared with controls, whereas G+/LVH– only showed a tendency toward lower septal peak diastolic circumferential strain rate compared with controls (Table 2). Lateral peak diastolic circumferential strain rate in G+/LVH+ and G+/LVH– was comparable to controls (Table 2).

Overall, the anatomical and functional characteristics show no differences between G+/LVH– compared with controls, whereas the G+/LVH+ group shows cardiac changes that are characteristic for HCM, such as increased LV mass, higher LV ejection fraction, lower septal peak SCS, and fibrosis.

Reduced Myocardial Efficiency at Preclinical and HCM Disease Stage in *TNNT2* Gene Variant Carriers

Figure 1 shows representative images of CMR and PET in the 3 groups. EW was similar in G+/LVH+ and controls, whereas it tended to be lower in G+/LVH– (Figure 4). Total MVO_2 was significantly higher in G+/LVH+ compared with controls and G+/LVH–, which is explained by the higher LV mass in G+/LVH+ (Figure 4).

Table 1. Baseline Characteristics

Characteristic	Controls (n=14)	G+/LVH− (n=6)	G+/LVH+ (n=8)
Genotype			
c.277G>A; p.Glu93Lys	…	1	1
c.304C>T, p.Arg102Trp	…	3	1
c.403C>T, p.Arg144Trp	…	1	0
c.832C>T p.Arg278Cys	…	0	1
c.835C>T; p.Gln279*	…	0	1
c.853C>T, p.Arg285Cys	…	0	1
c.856C>T, p.Arg286Cys	No gene variant	1	3
Age, y	48±11	43±15	46±16
Sex (men)	9	0*,†	7†
Body surface area, m^2	2.0±0.2	1.8±0.2	2.1±0.3†
Heart rate, beats/min	69±10	62±6	57±7*
Systolic blood pressure, mm Hg	123±13	114±14	123±15
Diastolic blood pressure, mm Hg	71±8	73±12	77±10
Mean arterial pressure, mm Hg	88±8	86±12	92±11
Medical treatment, n (%)			
β Blockers	0 (0)	0 (0)	2 (25)
Calcium antagonist	0 (0)	0 (0)	2 (25)
ACE inhibitors	0 (0)	0 (0)	2 (25)
Metabolic parameters			
k2	0.08±0.02	0.11±0.02*	0.08±0.01†
Hemoglobin, $mmol{\cdot}L^{-1}$	8.3±0.4	8.8±0.5	9.4±0.9*
NT-proBNP, $ng{\cdot}L^{-1}$	63±55	95±65	294±178*,†
Free fatty acids, $mmol{\cdot}L^{-1}$	0.55±0.26	0.67±0.20	0.49±0.27
Lactate, $mmol{\cdot}L^{-1}$	1.4±0.6	1.3±0.6	1.1±0.3
Glucose, $mmol{\cdot}L^{-1}$	5.5±0.8	5.9±1.5	5.4±0.5
Echocardiographic parameters			
Septal e', $cm{\cdot}s^{-1}$	10.1±2.3	8.1±4.4	7.2±0.9
E/A ratio	1.4±0.3	1.5±1.0	1.3±0.2
Mean LVOT gradient, mm Hg	NA	NA	3±1
CMR parameters			
Maximal LV septal wall thickness, mm	7 (6–8)	9 (8–10)*	16 (15–16)*,†
LV lateral wall thickness, mm	6.0±0.9	6.8±0.8	9.4±1.4*,†
LV end-diastolic volume, $mL{\cdot}m^{-2}$	93±15	73±12*	90±14
LV end-systolic volume, $mL{\cdot}m^{-2}$	36±10	27±5	28±10
Forward stroke volume, mL	100±23	71±12*	96±28
LV ejection fraction, %	62±5	65±6	73±13*
LV mass, $g{\cdot}m^{-2}$	49±6	39±5	67±13*,†
Indexed LV septal wall thickness, $mm{\cdot}m^{-2}$	3.5±0.4	5.1±0.6*	7.7±1.1*,†
Septal/lateral wall ratio	1.2±0.1	1.3±0.1	1.8±0.3*,†
Late gadolinium enhancement, n (%)	0 (0)	0 (0)	7 (11±10)

Data are presented as number, mean±SD, or median (interquartile range). ACE indicates angiotensin-converting enzyme; CMR, cardiac magnetic resonance; E/A, early to late ventricular filling velocities; e', early diastolic mitral annular velocity; G+/LVH+, genotype positive/left ventricular hypertrophy positive; G+/LVH−, genotype positive/left ventricular hypertrophy negative; k2, average [^{11}C]-acetate clearance rate constant; LV, left ventricular; LVOT, LV outflow tract; NA, not applicable; and NT-proBNP, N-terminal pro-B-type natriuretic peptide.

*$P<0.05$ vs controls.

†$P<0.05$ vs G+/LVH−.

Calculation of MEE revealed significantly lower values in G+/LVH− and G+/LVH+ compared with controls (Figure 4), indicative for reduced cardiac efficiency at preclinical disease stage.

Septal Versus Lateral LV Wall Changes in Efficiency of the HCM Heart

As hypertrophy specifically develops in the septum of the LV, we assessed regional efficiency to establish if reduced MEE is more severe in the septal than in the lateral wall of the LV. Figure 5 shows that septal and lateral myocardial efficiency, the ratio between peak $SCS/MVO_{2(beat)}$, were significantly lower (ie, less negative values) in G+/LVH− and G+/LVH+ compared with controls. The reduction in efficiency was similar in the septal and lateral wall of the LV both at preclinical and HCM disease stage. The reduction in efficiency at preclinical disease stage is explained by a significantly higher regional MVO_2 as no significant difference is present in regional peak SCS. A similar pattern is observed in the lateral wall of G+/LVH+ individuals with a significantly higher oxygen consumption and unaltered systolic strain compared with controls. The reduction in septal efficiency in G+/LVH+ compared with controls is explained by significantly lower systolic strain and the hypertrophy (LV mass)–related increase in oxygen consumption. Notably, septal oxygen consumption in G+/LVH+ did not differ from controls, and was significantly lower compared with G+/LVH−, indicative for a remodeling-related change in the hypertrophied septum of the G+/LVH+ group.

DISCUSSION

Using advanced cardiac PET and CMR imaging, we show reduced cardiac efficiency at preclinical and HCM disease stage in individuals carrying a *TNNT2* gene variant. The lower MEE in G+/LVH− is explained by higher global and regional oxygen consumption compared with healthy controls. Regional analysis showed significantly higher MVO_2 in the septal and lateral LV wall of G+/LVH− and the lateral wall of G+/LVH+ compared with controls, indicating that the presence of a *TNNT2* gene variant increases local oxygen consumption and reduces efficiency of cardiac contraction. The reduced septal efficiency in the HCM group is explained by the increase in LV mass and concomitant higher oxygen consumption and reduced systolic strain. Septal oxygen consumption was significantly lower in G+/LVH+ compared with G+/LVH−, suggesting that disease mechanisms other than the gene variant alter oxygen consumption and/or delivery in the hypertrophied myocardium. No significant changes in regional contractile parameters, both systolic and diastolic, were observed at

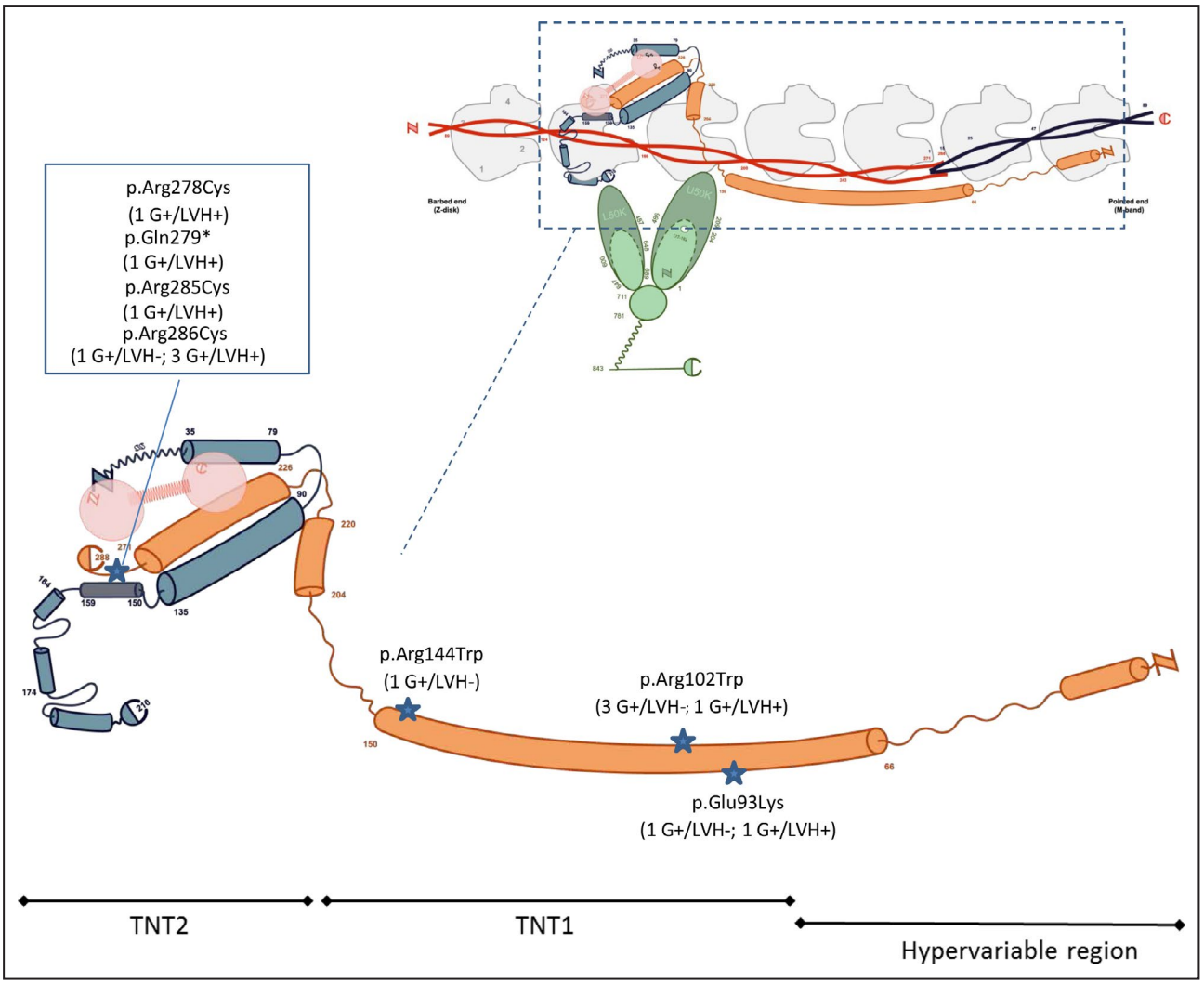

Figure 3. Schematic figure of locations of *TNNT2* (troponin T gene) variants.
Schematic of the thin filament composed of actin, tropomyosin, and the troponin complex, and myosin head of the thick filament (depicted in green). Seven actin monomers (gray) spanned by 1 tropomyosin dimer (red) and 1 troponin complex: cardiac troponin C (pink), cardiac troponin I (blue), and cardiac troponin T (orange). Dark-blue tropomyosin depicts near-neighbor tropomyosin dimer interaction. The *TNNT2* gene variants detected in 6 genotype-positive/left ventricular hypertrophy–negative (G+/LVH–) and 8 genotype-positive/left ventricular hypertrophy–positive (G+/LVH+) study subjects are depicted relative to their location in the troponin T protein. Based on the figure shown with permission from Sequeira et al.[30] Copyright ©2015, Springer Nature. C indicates C-terminal protein end; N, N-terminal protein end. Troponin T can be divided in three sub-regions: the N-terminal hypervariable region, TNT1 and the C-terminal TNT2.

preclinical disease stage. Although LV ejection fraction was significantly higher in patients with HCM, both systolic and diastolic strain parameters were lower compared with controls, which was most evident in the hypertrophied septal wall of the LV. Our data show that the increase in MVO_2 in *TNNT2* gene variant carriers precedes changes in global and regional myocardial contractility, indicating that the energetic status rather than contractile parameters reflects the initial variant-induced pathomechanism that can be used for early diagnosis and preventive therapy. The combination of reduced strain, increased NT-proBNP levels, and reduced peak diastolic strain rate indicates progression of disease in G+/LVH+ patients compared with G+/LVH–. In this respect, the reduction (pseudonormalization) of MVO_2 observed in this study is in line with energy depletion also observed in patients with HCM and patients with heart failure.

Reduced Myocardial Efficiency Caused by Different Variants in *TNNT2*

Cardiac troponin T is part of the thin filament of the sarcomere, which is composed of actin, tropomyosin, and the troponin complex (Figure 3). Together with

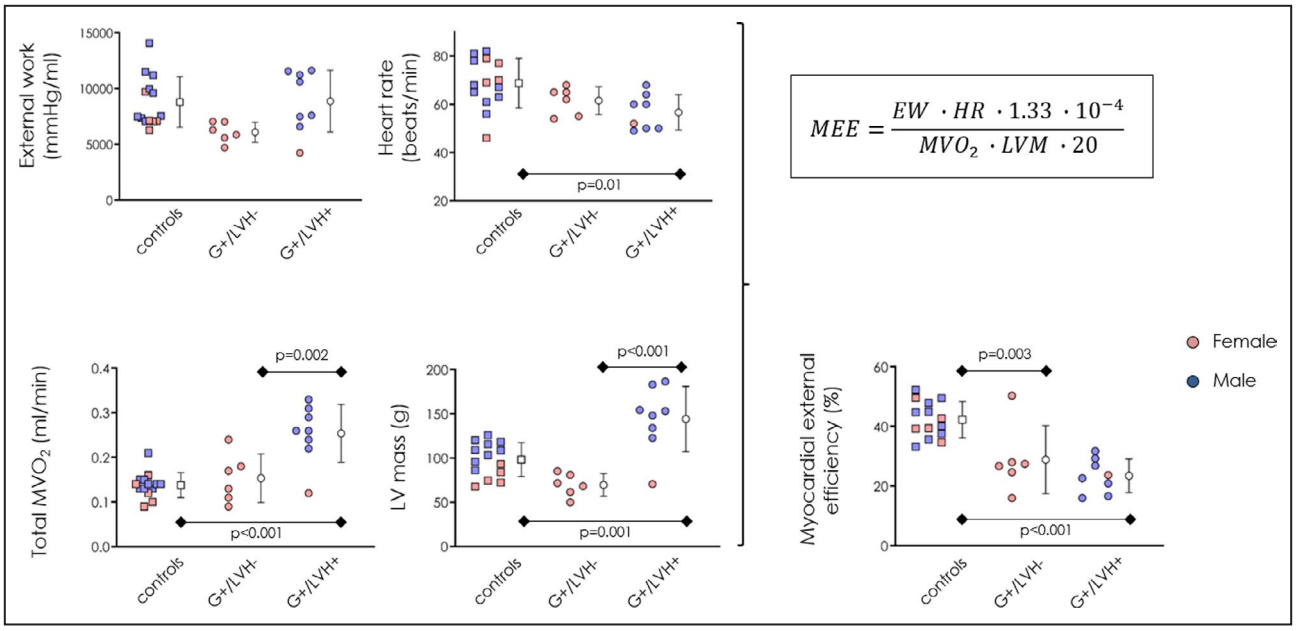

Figure 4. Reduced myocardial external efficiency at preclinical and hypertrophic cardiomyopathy (HCM) disease stage. Scatterplots depict external work (EW), heart rate (HR), total myocardial oxygen consumption (MVO_2), left ventricular mass (LVM), and myocardial external efficiency (MEE) in controls, genotype positive/left ventricular hypertrophy negative (G+/LVH–), and genotype positive/left ventricular hypertrophy positive (G+/LVH+). EW was similar in G+/LVH+ and controls, but tended to be lower in G+/LVH–. Total MVO_2 was higher in G+/LVH+ compared with controls and G+/LVH–, which is explained by the higher LVM in G+/LVH+. Calculation of MEE revealed significantly lower values in G+/LVH– and G+/LVH+ compared with controls, indicative for reduced cardiac efficiency at early preclinical disease stage. MEE was similar at preclinical (G+/LVH–) and HCM (G+/LVH+) disease stage. Data are presented as mean with SD.

cardiac troponin I and cardiac troponin C, cardiac troponin T forms the Ca^{2+}-regulatory troponin complex of the thin filament. Activation of cardiomyocytes induces an increase in cytosolic [Ca^{2+}] and Ca^{2+} binding to cardiac troponin C, which changes the conformation of the troponin-tropomyosin complex, and exposes myosin-binding sites on actin. Increased binding of myosin heads to the actin thin filament (formation of cross-bridges) subsequently generates force. The troponin complex is thus a central player in cardiomyocyte force development during the systolic and diastolic phase of the cardiac cycle. On the basis of its central role in myofilament Ca^{2+} signaling and contractility, variants in *TNNT2* are likely to alter myofilament properties. Several myofilament changes caused by *TNNT2* variants have been reported that may underlie increased energy (oxygen) consumption and the reduction in myocardial efficiency. A common feature of myofilaments harboring *TNNT2* variants is increased myofilament Ca^{2+} sensitivity, which coincides with increased ATPase activity.[18,32]

Ca^{2+}-activated human myofilaments harboring a *TNNT2* variant showed higher cross-bridge kinetics, increased tension cost (ie, higher ATP use for force development), and a blunted length-dependent activation compared with nonfailing control tissue.[11,33] The higher myofilament Ca^{2+} sensitivity and increased cross-bridge kinetics may underlie reduced MEE in preclinical G+/LVH–. In addition, the blunted length-dependent activation of myofilaments with a *TNNT2* gene variant represents a highly inefficient myofilament

Table 2. Regional Contractile Function and Efficiency

Variable	Controls (n=14)	G+/LVH– (n=6)	G+/LVH+ (n=8)
Peak systolic circumferential strain, %			
Global	–17.5±1.4	–18.8±2.5	–15.5±2.2*,†
Septal	–16.2±2.2	–16.8±2.5	–13.3±2.7*,†
Lateral	–19.0±2.0	–20.8±2.7	–18.5±2.3
Peak diastolic circumferential strain rate, %·s^{-1}			
Global	38.3±7.0	32.0±5.2	28.7±6.8
Septal	38.2±8.7	30.9±7.5	24.6±7.2*
Lateral	40.8±7.5	34.6±5.7	37.0±6.7
MVO_2 per beat, mL/beat per g·10^{-3}			
Global	1.4±0.3	2.2±0.4*	1.7±0.2*,†
Septal	1.4±0.3	2.3±0.4*	1.7±0.2†
Lateral	1.4±0.3	2.3±0.5*	1.9±0.2*
Efficiency (systolic circumferential strain/MVO_2 per beat)			
Global	–12 009±1797	–8458±2048*	–8047±1379*
Septal	–11 413±1430	–7666±1968*	–7744±1856*
Lateral	–13 625±2752	–9633±2464*	–9841±1617*

Data are presented as mean±SD. G+/LVH+ indicates genotype positive/left ventricular hypertrophy positive; G+/LVH–, genotype positive/left ventricular hypertrophy negative; and MVO_2, myocardial oxygen consumption.

*P<0.05 vs controls.

†P<0.05 vs G+/LVH– individuals.

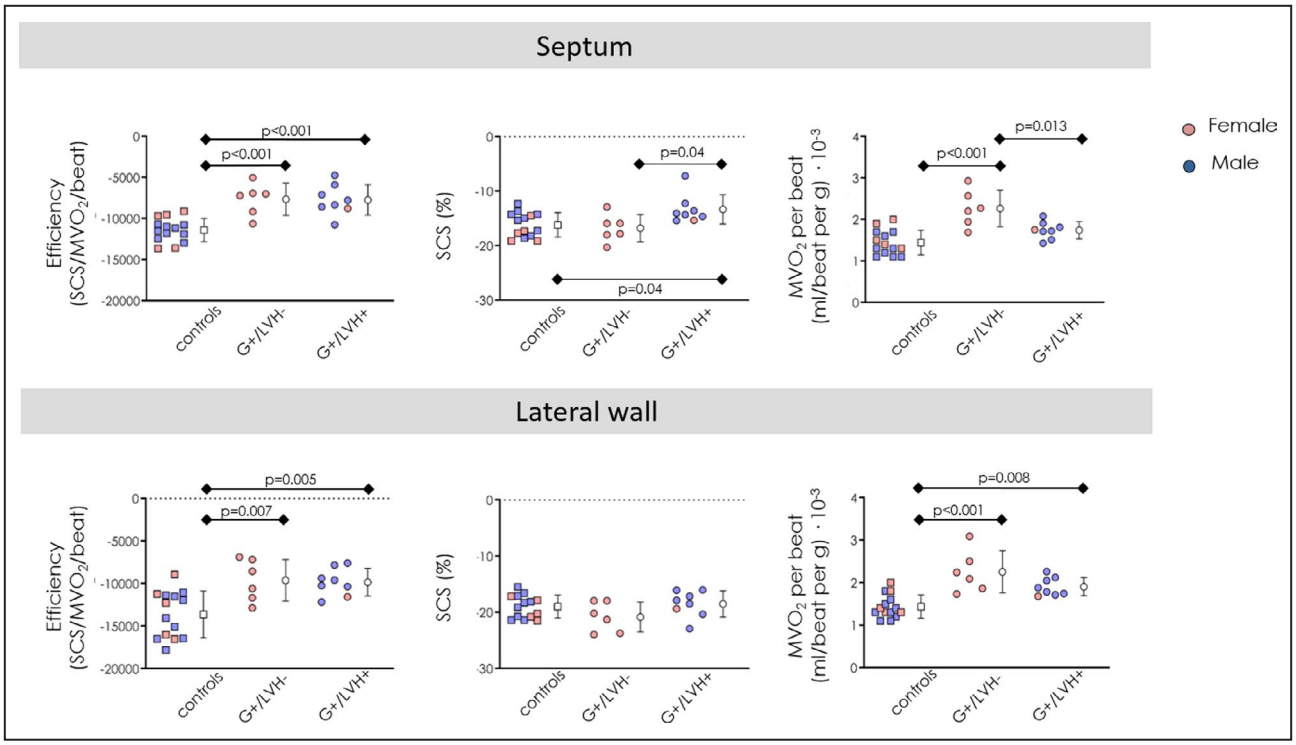

Figure 5. Cardiac efficiency, regional contractility and oxygen consumption.
Septal and lateral myocardial efficiency were significantly lower in genotype positive/left ventricular hypertrophy negative (G+/LVH–) and genotype positive/left ventricular hypertrophy positive (G+/LVH+) compared with controls. The scatterplots depicting systolic circumferential strain (SCS) and myocardial oxygen consumption (MVO_2) illustrate which regional changes cause the reduction in septal and lateral efficiency. Data are presented as mean with SD.

mechanism. Studies in HCM mouse models showed large differences in the variant-dependent increase in myofilament Ca^{2+} sensitivity, with the I79N variant causing the largest increase, and the R92Q variant having no significant effect.[34] Our study population carried variants in different parts of the *TNNT2* gene. Cardiac troponin T can be divided in 3 subregions: the N-terminal hypervariable region (residues 1–79), TNT1 (residues 80–180), and the C-terminal TNT2 (residues 181–288; Figure 3).[35,36] Gene variants located in the TNT1 region result in a reduced affinity of cardiac troponin T for tropomyosin, whereas C-terminus gene variants do not alter this interaction, suggesting variant location-dependent pathomechanisms.[37,38] Most of the *TNNT2* variants in our G+/LVH+ group are located in the TNT2 region, whereas in 5 of 6 G+/LVH–, the variant is located in the TNT1 region (Figure 3). Although the location of the variant may underlie its pathomechanism and pathogenicity, we did not observe a difference in MEE between variants located in TNT1 and TNT2 as MEE is similarly reduced in individuals with TNT1 and TNT2 gene variants (Figure 4). Prospective imaging studies are warranted in young (aged 20–45 years) male and female TNT1 and TNT2 variant carriers to establish if the variant-mediated reduction in MEE has prognostic relevance.

Limitations and Clinical Implications

Sex differences

We used the current European Society of Cardiology guidelines to classify the gene variant carriers into a G+/LVH– group and a G+/LVH+ group. A significant sex difference in the distribution of women and men in the 2 groups is present, which may be partly explained by using a cutoff value for septal thickness that is uncorrected for body surface area (BSA). In recent studies, we highlighted the importance of correcting septal thickness by BSA as women are in general smaller than men.[31,39] When we do take into account differences in BSA in the present study, indexed LV septal wall thickness is significantly higher in the female G+/LVH– group (5.1±0.6; Table 1) compared with female controls (3.5±0.4; Table S1). The increase in indexed septal wall thickness in female G+/LVH– compared with female controls is 45%, whereas the increase in indexed septal wall thickness in male patients with HCM (7.7±1.1; Table 1) compared with male controls (3.5±0.5; Table S1) is 120%. The latter supports the more advanced remodeling in the G+/LVH+ group, although it also emphasizes the need to correct septal thickness and LV mass for BSA, and necessitates a reappraisal of the definition of hypertrophy in HCM.

BSA-corrected values for MEE and septal oxygen consumption are shown in Figure S1, and illustrate a similar pattern as the uncorrected values (Figures 4 and 5). Overall, our study indicates that future studies on cardiac remodeling should take into account differences in BSA as they may explain sex-specific differences in disease cardiac remodeling and disease progression.

Remodeling-related changes in cardiac efficiency

In addition to the variant-induced functional changes in the heart, additional disease mechanisms may underlie the reduction in MEE, such as capillary rarefaction,[40] microvascular (endothelial) dysfunction,[41] mitochondrial dysfunction, and oxidative stress.[42] Coronary flow reserve may underlie changes in MEE, and has been proposed as disease marker for HCM independent of the severity of LV hypertrophy.[43] The blunted vasodilator reserve in the absence of a coronary stenosis in HCM is the result of microvascular dysfunction.[41] Pharmacologically induced coronary vasodilation was significantly impaired in the hypertrophied septal and nonhypertrophied free wall of patients with HCM,[44] showing that vascular (endothelial) dysfunction is independent of cardiac hypertrophy. In a previous study, we did not find impaired vascular reserve in *MYBPC3* G+/LVH– and reduced MEE.[23] Studies to define regional coronary flow reserve at different stages of HCM with different genotypes are warranted to define the role of impaired coronary vasodilation in the pathogenesis of HCM with respect to changes in cardiac efficiency and metabolism. In addition to microvascular changes, increased interstitial fibrosis, a marker of cardiac ischemia, may contribute to inefficient cardiac function. Because the current study participants did not undergo cardiac catheterization to exclude coronary artery disease before enrollment, myocardial ischemia attributable to coronary artery disease could potentially influence the current results. However, this study has a limited sample size, participants were asymptomatic and at low risk to experience coronary artery disease, and electrocardiography did not reveal abnormalities attributable to ischemic cardiac disease. Myocardial metabolism was derived by the clearance rate of carbon-11 acetate, which can only be measured in viable myocardium. Analysis of extracellular volume using CMR with LGE images (Table 1) showed no LGE in G+/LVH–, indicating that a change in regional extracellular volume does not influence their energetic phenotype. Because G+/LVH+ individuals presented with limited scar tissue on CMR (Table 1), and thus have limited nonviable myocardium, we did not correct MEE for scar tissue in our analyses. The effect of extracellular volume on regional contractile function was shown to be limited,[45] and therefore extracellular volume measurement was not performed in this study. However, the interaction between in vivo measured myocardial structure and regional function still warrants further study.

Treatment options

Currently, there are no preventive or curative therapies for HCM. Metabolic modulators have been proposed to correct energy deficiency.[46] In animal and human studies, metabolic modulators, such as trimetazidine and perhexiline, have a proven positive effect on energy efficiency and have improved diastolic function and exercise capacity.[47,48] Perhexiline improved exercise capacity in patients with obstructive HCM,[46] whereas a recent study in patients with HCM did not show a beneficial effect of trimetazidine.[49] Effectiveness of therapies may depend on the affected gene, as has been shown by Ho et al, who showed a positive effect of diltiazem only in preclinical *MYBPC3* gene variant carriers.[50] Thus far, clinical trials in patients with HCM with metabolic modulators have been performed in mixed groups of patients with HCM with and without (known) gene variants. Moreover, our study indicates that the effectiveness of metabolic therapy may depend on disease stage as oxygen consumption is not increased in the hypertrophied septal region of the LV in HCM. Alternative attractive strategies to lower oxygen consumption are therapies that aim to lower contractility of the heart muscle.[51] A recent proof-of-concept study performed in symptomatic patients with HCM revealed significant reduction of LV outflow tract gradient and improvement of exercise capacity with a 12-week treatment with mavacamten, which is suggested to attenuate hypercontractile myofilaments, and therefore should be investigated further as a potential treatment in patients with HCM.[52] To come to disease stage-specific and even gene-specific treatment strategies, more knowledge is needed about the pathomechanisms underlying reduced MEE. Follow-up studies are warranted to investigate the mechanisms (ie, metabolism, mitochondrial function, and vascular responsiveness) underlying the changes in oxygen consumption and delivery during the transition from preclinical nonhypertrophied disease stage to manifest obstructive HCM.

In conclusion, our study shows that preclinical gene variant carriers have an initial increase in oxygen consumption preceding cardiac hypertrophy and contractile dysfunction, suggesting that high oxygen consumption and reduced MEE characterize the early disease mechanisms that may be used for early diagnosis and development of preventive treatments.

ARTICLE INFORMATION

Received December 3, 2019; accepted February 25, 2020.

Affiliations

From the Departments of Cardiology (R.Y.P., A.C.v.R., T.G.) and Physiology (R.Y.P., J.v.d.V.), Amsterdam University Medical Center, Amsterdam Cardiovascular Sciences, Vrije Universiteit University Medical Center Amsterdam, Amsterdam, The Netherlands; Department of Cardiology, Erasmus Medical Center, Rotterdam, The Netherlands (M.M.); The Netherlands Heart Institute, Utrecht, The Netherlands (R.Y.P., J.v.d.V.); and Department of Nuclear Medicine and PET Center Aarhus University, Aarhus, Denmark (H.J.H.).

Acknowledgments

The authors thank Peter van de Ven for the statistical analyses; and Daniela Barge-Schaapveld, Anneke van Mil, Hannah G. van Velzen, Dennis Dooijes, Arjan Houweling, Peter van Tintelen, and Freyja van Lint for screening *TNNT2* gene variant individuals. We thank Vasco Sequeira for the design of Figure 3.

Sources of Funding

This work was supported by The Netherlands Heart Foundation (CVON-Dosis 2014–40) and Netherlands Organization for Sciences-ZonMW (VICI 91818602).

Disclosures

None.

Supplementary Material

Data S1
Table S1
Figure S1
References 22, 28, 53 and 54

REFERENCES

1. Semsarian C, Ingles J, Maron MS, Maron BJ. New perspectives on the prevalence of hypertrophic cardiomyopathy. *J Am Coll Cardiol*. 2015;65:1249–1254.
2. Authors/Task Force members, Elliott PM, Anastasakis A, Borger MA, Borggrefe M, Cecchi F, Charron P, Hagege AA, Lafont A, Limongelli G, Mahrholdt H, et al. 2014 ESC guidelines on diagnosis and management of hypertrophic cardiomyopathy: the Task Force for the Diagnosis and Management of Hypertrophic Cardiomyopathy of the European Society of Cardiology (ESC). *Eur Heart J*. 2014;35:2733–2779.
3. Ho CY, Charron P, Richard P, Girolami F, Van Spaendonck-Zwarts KY, Pinto Y. Genetic advances in sarcomeric cardiomyopathies: state of the art. *Cardiovasc Res*. 2015;105:397–408.
4. Marian AJ, Roberts R. The molecular genetic basis for hypertrophic cardiomyopathy. *J Mol Cell Cardiol*. 2001;33:655–670.
5. Coppini R, Ho CY, Ashley E, Day S, Ferrantini C, Girolami F, Tomberli B, Bardi S, Torricelli F, Cecchi F, et al. Clinical phenotype and outcome of hypertrophic cardiomyopathy associated with thin-filament gene mutations. *J Am Coll Cardiol*. 2014;64:2589–2600.
6. Van Driest SL, Ellsworth EG, Ommen SR, Tajik AJ, Gersh BJ, Ackerman MJ. Prevalence and spectrum of thin filament mutations in an outpatient referral population with hypertrophic cardiomyopathy. *Circulation*. 2003;108:445–451.
7. Moolman JC, Corfield VA, Posen B, Ngumbela K, Seidman C, Brink PA, Watkins H. Sudden death due to troponin T mutations. *J Am Coll Cardiol*. 1997;29:549–555.
8. Watkins H, McKenna WJ, Thierfelder L, Suk HJ, Anan R, O'Donoghue A, Spirito P, Matsumori A, Moravec CS, Seidman JG, et al. Mutations in the genes for cardiac troponin T and alpha-tropomyosin in hypertrophic cardiomyopathy. *N Engl J Med*. 1995;332:1058–1064.
9. van Velzen HG, Vriesendorp PA, Oldenburg RA, van Slegtenhorst MA, van der Velden J, Schinkel AFL, Michels M. Value of genetic testing for the prediction of long-term outcome in patients with hypertrophic cardiomyopathy. *Am J Cardiol*. 2016;118:881–887.
10. Ferrantini C, Coppini R, Pioner JM, Gentile F, Tosi B, Mazzoni L, Scellini B, Piroddi N, Laurino A, Santini L, et al. Pathogenesis of hypertrophic cardiomyopathy is mutation rather than disease specific: a comparison of the cardiac troponin T E163R and R92Q mouse models. *J Am Heart Assoc*. 2017;6:e005407. DOI: 10.1161/JAHA.116.005407.
11. Sequeira V, Wijnker PJ, Nijenkamp LL, Kuster DW, Najafi A, Witjas-Paalberends ER, Regan JA, Boontje N, Ten Cate FJ, Germans T, et al. Perturbed length-dependent activation in human hypertrophic cardiomyopathy with missense sarcomeric gene mutations. *Circ Res*. 2013;112:1491–1505.
12. Robinson P, Liu X, Sparrow A, Patel S, Zhang YH, Casadei B, Watkins H, Redwood C. Hypertrophic cardiomyopathy mutations increase myofilament Ca(2+) buffering, alter intracellular Ca(2+) handling, and stimulate Ca(2+)-dependent signaling. *J Biol Chem*. 2018;293:10487–10499.
13. Hernandez OM, Szczesna-Cordary D, Knollmann BC, Miller T, Bell M, Zhao J, Sirenko SG, Diaz Z, Guzman G, Xu Y, et al. F110I and R278C troponin T mutations that cause familial hypertrophic cardiomyopathy affect muscle contraction in transgenic mice and reconstituted human cardiac fibers. *J Biol Chem*. 2005;280:37183–37194.
14. Javadpour MM, Tardiff JC, Pinz I, Ingwall JS. Decreased energetics in murine hearts bearing the R92Q mutation in cardiac troponin T. *J Clin Invest*. 2003;112:768–775.
15. Spindler M, Saupe KW, Christe ME, Sweeney HL, Seidman CE, Seidman JG, Ingwall JS. Diastolic dysfunction and altered energetics in the alphaMHC403/+ mouse model of familial hypertrophic cardiomyopathy. *J Clin Invest*. 1998;101:1775–1783.
16. Jung WI, Sieverding L, Breuer J, Hoess T, Widmaier S, Schmidt O, Bunse M, van Erckelens F, Apitz J, Lutz O, et al. 31P NMR spectroscopy detects metabolic abnormalities in asymptomatic patients with hypertrophic cardiomyopathy. *Circulation*. 1998;97:2536–2542.
17. Crilley JG, Boehm EA, Blair E, Rajagopalan B, Blamire AM, Styles P, McKenna WJ, Ostman-Smith I, Clarke K, Watkins H. Hypertrophic cardiomyopathy due to sarcomeric gene mutations is characterized by impaired energy metabolism irrespective of the degree of hypertrophy. *J Am Coll Cardiol*. 2003;41:1776–1782.
18. Witjas-Paalberends ER, Guclu A, Germans T, Knaapen P, Harms HJ, Vermeer AM, Christiaans I, Wilde AA, Dos Remedios C, Lammertsma AA, et al. Gene-specific increase in the energetic cost of contraction in hypertrophic cardiomyopathy caused by thick filament mutations. *Cardiovasc Res*. 2014;103:248–257.
19. Guclu A, Knaapen P, Harms HJ, Parbhudayal RY, Michels M, Lammertsma AA, van Rossum AC, Germans T, van der Velden J. Disease stage-dependent changes in cardiac contractile performance and oxygen utilization underlie reduced myocardial efficiency in human inherited hypertrophic cardiomyopathy. *Circ Cardiovasc Imaging*. 2017;10:e005604.
20. Tardiff JC, Carrier L, Bers DM, Poggesi C, Ferrantini C, Coppini R, Maier LS, Ashrafian H, Huke S, van der Velden J. Targets for therapy in sarcomeric cardiomyopathies. *Cardiovasc Res*. 2015;105:457–470.
21. Cheitlin MD, Armstrong WF, Aurigemma GP, Beller GA, Bierman FZ, Davis JL, Douglas PS, Faxon DP, Gillam LD, Kimball TR, et al. ACC/AHA/ASE 2003 guideline update for the clinical application of echocardiography: summary article: a report of the American College of Cardiology/American Heart Association Task Force on Practice Guidelines (ACC/AHA/ASE Committee to Update the 1997 Guidelines for the Clinical Application of Echocardiography). *Circulation*. 2003;108:1146–1162.
22. Sun KT, Yeatman LA, Buxton DB, Chen K, Johnson JA, Huang SC, Kofoed KF, Weismueller S, Czernin J, Phelps ME, et al. Simultaneous measurement of myocardial oxygen consumption and blood flow using [1-carbon-11]acetate. *J Nucl Med*. 1998;39:272–280.
23. Timmer SA, Germans T, Brouwer WP, Lubberink M, van der Velden J, Wilde AA, Christiaans I, Lammertsma AA, Knaapen P, van Rossum AC. Carriers of the hypertrophic cardiomyopathy MYBPC3 mutation are characterized by reduced myocardial efficiency in the absence of hypertrophy and microvascular dysfunction. *Eur J Heart Fail*. 2011;13:1283–1289.
24. Swoboda PP, Larghat A, Zaman A, Fairbairn TA, Motwani M, Greenwood JP, Plein S. Reproducibility of myocardial strain and left ventricular twist measured using complementary spatial modulation of magnetization. *J Magn Reson Imaging*. 2014;39:887–894.
25. Arts T, Prinzen FW, Delhaas T, Milles JR, Rossi AC, Clarysse P. Mapping displacement and deformation of the heart with local sine-wave modeling. *IEEE Trans Med Imaging*. 2010;29:1114–1123.
26. Cerqueira MD, Weissman NJ, Dilsizian V, Jacobs AK, Kaul S, Laskey WK, Pennell DJ, Rumberger JA, Ryan T, Verani MS, et al. Standardized

myocardial segmentation and nomenclature for tomographic imaging of the heart: a statement for healthcare professionals from the Cardiac Imaging Committee of the Council on Clinical Cardiology of the American Heart Association. *Circulation*. 2002;105:539–542.
27. Flett AS, Hasleton J, Cook C, Hausenloy D, Quarta G, Ariti C, Muthurangu V, Moon JC. Evaluation of techniques for the quantification of myocardial scar of differing etiology using cardiac magnetic resonance. *JACC Cardiovasc Imaging*. 2011;4:150–156.
28. Harms HJ, Knaapen P, de Haan S, Halbmeijer R, Lammertsma AA, Lubberink M. Automatic generation of absolute myocardial blood flow images using [^{15}O]H_2O and a clinical PET/CT scanner. *Eur J Nucl Med Mol Imaging*. 2011;38:930–939.
29. Knaapen P, Germans T, Knuuti J, Paulus WJ, Dijkmans PA, Allaart CP, Lammertsma AA, Visser FC. Myocardial energetics and efficiency: current status of the noninvasive approach. *Circulation*. 2007;115:918–927.
30. Sequeira V, van der Velden J. Historical perspective on heart function: the Frank-Starling Law. *Biophys Rev*. 2015;7:421–447.
31. van Driel B, Nijenkamp L, Huurman R, Michels M, van der Velden J. Sex differences in hypertrophic cardiomyopathy: new insights. *Curr Opin Cardiol*. 2019;34:254–259.
32. Robinson P, Griffiths PJ, Watkins H, Redwood CS. Dilated and hypertrophic cardiomyopathy mutations in troponin and alpha-tropomyosin have opposing effects on the calcium affinity of cardiac thin filaments. *Circ Res*. 2007;101:1266–1273.
33. Piroddi N, Witjas-Paalberends ER, Ferrara C, Ferrantini C, Vitale G, Scellini B, Wijnker PJM, Sequiera V, Dooijes D, Dos Remedios C, et al. The homozygous K280N troponin T mutation alters cross-bridge kinetics and energetics in human HCM. *J Gen Physiol*. 2019;151:18–29.
34. Knollmann BC, Potter JD. Altered regulation of cardiac muscle contraction by troponin T mutations that cause familial hypertrophic cardiomyopathy. *Trends Cardiovasc Med*. 2001;11:206–212.
35. Jin JP, Chong SM. Localization of the two tropomyosin-binding sites of troponin T. *Arch Biochem Biophys*. 2010;500:144–150.
36. Tardiff JC. Thin filament mutations: developing an integrative approach to a complex disorder. *Circ Res*. 2011;108:765–782.
37. Moore RK, Abdullah S, Tardiff JC. Allosteric effects of cardiac troponin TNT1 mutations on actomyosin binding: a novel pathogenic mechanism for hypertrophic cardiomyopathy. *Arch Biochem Biophys*. 2014;552–553:21–28.
38. Gangadharan B, Sunitha MS, Mukherjee S, Chowdhury RR, Haque F, Sekar N, Sowdhamini R, Spudich JA, Mercer JA. Molecular mechanisms and structural features of cardiomyopathy-causing troponin T mutants in the tropomyosin overlap region. *Proc Natl Acad Sci USA*. 2017;114:11115–11120.
39. Nijenkamp L, Bollen IAE, van Velzen HG, Regan JA, van Slegtenhorst M, Niessen HWM, Schinkel AFL, Kruger M, Poggesi C, Ho CY, et al. Sex differences at the time of myectomy in hypertrophic cardiomyopathy. *Circ Heart Fail*. 2018;11:e004133.
40. Guclu A, Happe C, Eren S, Korkmaz IH, Niessen HW, Klein P, van Slegtenhorst M, Schinkel AF, Michels M, van Rossum AC, et al. Left ventricular outflow tract gradient is associated with reduced capillary density in hypertrophic cardiomyopathy irrespective of genotype. *Eur J Clin Invest*. 2015;45:1252–1259.
41. Olivotto I, Girolami F, Sciagra R, Ackerman MJ, Sotgia B, Bos JM, Nistri S, Sgalambro A, Grifoni C, Torricelli F, et al. Microvascular function is selectively impaired in patients with hypertrophic cardiomyopathy and sarcomere myofilament gene mutations. *J Am Coll Cardiol*. 2011;58:839–848.
42. Christiansen LB, Dela F, Koch J, Hansen CN, Leifsson PS, Yokota T. Impaired cardiac mitochondrial oxidative phosphorylation and enhanced mitochondrial oxidative stress in feline hypertrophic cardiomyopathy. *Am J Physiol Heart Circ Physiol*. 2015;308:H1237–H1247.
43. Choudhury L, Elliott P, Rimoldi O, Ryan M, Lammertsma AA, Boyd H, McKenna WJ, Camici PG. Transmural myocardial blood flow distribution in hypertrophic cardiomyopathy and effect of treatment. *Basic Res Cardiol*. 1999;94:49–59.
44. Camici P, Chiriatti G, Lorenzoni R, Bellina RC, Gistri R, Italiani G, Parodi O, Salvadori PA, Nista N, Papi L, L'Abbate A. Coronary vasodilation is impaired in both hypertrophied and nonhypertrophied myocardium of patients with hypertrophic cardiomyopathy: a study with nitrogen-13 ammonia and positron emission tomography. *J Am Coll Cardiol*. 1991;17:879–886.
45. Swoboda PP, McDiarmid AK, Erhayiem B, Law GR, Garg P, Broadbent DA, Ripley DP, Musa TA, Dobson LE, Foley JR, et al. Effect of cellular and extracellular pathology assessed by T1 mapping on regional contractile function in hypertrophic cardiomyopathy. *J Cardiovasc Magn Reson*. 2017;19:16.
46. Abozguia K, Elliott P, McKenna W, Phan TT, Nallur-Shivu G, Ahmed I, Maher AR, Kaur K, Taylor J, Henning A, et al. Metabolic modulator perhexiline corrects energy deficiency and improves exercise capacity in symptomatic hypertrophic cardiomyopathy. *Circulation*. 2010;122:1562–1569.
47. Stanley WC, Recchia FA, Lopaschuk GD. Myocardial substrate metabolism in the normal and failing heart. *Physiol Rev*. 2005;85:1093–1129.
48. Lee L, Horowitz J, Frenneaux M. Metabolic manipulation in ischaemic heart disease, a novel approach to treatment. *Eur Heart J*. 2004;25:634–641.
49. Coats CJ, Pavlou M, Watkinson OT, Protonotarios A, Moss L, Hyland R, Rantell K, Pantazis AA, Tome M, McKenna WJ, et al. Effect of trimetazidine dihydrochloride therapy on exercise capacity in patients with non-obstructive hypertrophic cardiomyopathy: a randomized clinical trial. *JAMA Cardiol*. 2019;4:230–235.
50. Ho CY, Lakdawala NK, Cirino AL, Lipshultz SE, Sparks E, Abbasi SA, Kwong RY, Antman EM, Semsarian C, Gonzalez A, et al. Diltiazem treatment for pre-clinical hypertrophic cardiomyopathy sarcomere mutation carriers: a pilot randomized trial to modify disease expression. *JACC Heart Fail*. 2015;3:180–188.
51. van der Velden J, Tocchetti CG, Varricchi G, Bianco A, Sequeira V, Hilfiker-Kleiner D, Hamdani N, Leite-Moreira AF, Mayr M, Falcao-Pires I, et al. Metabolic changes in hypertrophic cardiomyopathies: scientific update from the Working Group of Myocardial Function of the European Society of Cardiology. *Cardiovasc Res*. 2018;114:1273–1280.
52. Heitner SB, Jacoby D, Lester SJ, Owens A, Wang A, Zhang D, Lambing J, Lee J, Semigran M, Sehnert AJ. Mavacamten treatment for obstructive hypertrophic cardiomyopathy: a clinical trial. *Ann Intern Med*. 2019;170:741–748.
53. Marcus JT, DeWaal LK, Gotte MJ, van der Geest RJ, Heethaar RM, Van Rossum AC. MRI-derived left ventricular function parameters and mass in healthy young adults: relation with gender and body size. *Int J Card Imaging*. 1999;15:411–419.
54. Zwanenburg JJ, Kuijer JP, Marcus JT, Heethaar RM. Steady-state free precession with myocardial tagging: CSPAMM in a single breathhold. *Magn Reson Med*. 2003;49:722–730.

Supplemental Material

Data S1.

Supplemental Methods

Cardiac Magnetic Resonance imaging

Image parameters were as follows: slice thickness 5 mm, slice gap 5 mm, temporal resolution <50 ms, repetition time 3.2 ms, echo time 1.54 ms, flip angle 60° and a typical image resolution of 1.3 by 1.6 mm. The cardiac cycle consisted of 20 phases. After obtaining 4-, 3-, and 2-chamber view cines, stacks of 10-12 short axis slices were acquired for full coverage of the left ventricle (LV).[53] A multiple breath-hold, retrospective triggered bSSFP myocardial sinusoidal complementary tagged (CSPAMM) images were acquired to create non-invasive markers (tags) within the myocardium.[54] Midventricular short axis planes were positioned at 25, 50 and 75 percent of the distance between the mitral valve annulus and the endocardial border of the apex. Image parameters: field of view: 300 × 300 mm2, flip-angle: 20°, repetition time: 3.6 ms, echo time: 1.8 ms, receiver bandwidth: 850 Hz/pixel, matrix size: 256 × 78, slice thickness: 6 mm, tag-line distance: 7 mm. Late gadolinium enhancement (LGE) images were acquired 10-15 minutes after intravenous administration of 0.2 mmol·kg^{-1} Gadolinium, using a two-dimensional segmented inversion-recovery prepared gradient-echo sequence. Inversion-recovery time was 250-300 ms.

[^{11}C]-acetate PET imaging and analysis

A 50 minute list-mode emission scan was started simultaneously with a bolus injection of 370 MBq of [^{11}C]-acetate (infusion speed 0.8 mL · s^{-1}) followed by a 35 mL saline flush (infusion speed 2 mL · s^{-1}). Correction for attenuation and scatter was achieved by a slow, respiration-averaged low dose CT scan (LD-CT, 55 mAs, rotation time 1.5 s, pitch 0.825, collimation 64x0.625, acquiring 20 cm in 12 s) during normal breathing after the emission scan. Data were reconstructed into 36 successive time frames (1x10, 8x5, 4x10, 3x20, 5x30, 5x60, 4x150, 6x300 s). Blood pressure and heart rate were

recorded at time of bolus injection and 5, 10 and 15 minutes after injection. In-house developed software facilitated analysis.[28] A correction for the fraction of non-metabolized [^{11}C]-acetate was applied to $C_A(t)$.[22]

Table S1. No sex-differences in myocardial external efficiency in control group.

	Controls		
	Male (n=9)	**Female (n=5)**	**p-value**
Mean arterial pressure (mmHg)	88 ± 8	89 ± 9	0.70
External work (mmHg·ml^{-1})	9537.13 ± 2410.46	7456.39 ± 1316.24	0.1
LV mass (g)	109 ± 13	78 ± 10	0.001
LV mass (g·m^{-2})	52 ± 4	42 ± 5	0.006
Indexed LV septal wall thickness (mm·m^{-2})	3.5 ± 0.5	3.5 ± 0.4	0.9
Stroke volume (ml)	124.7 ± 21.2	96.8 ± 12.3	0.009
Stroke volume (ml·m^{-2})	59 ± 8	52 ± 4	0.05
Peak systolic circumferential strain (%)			
Global	-17.1 ± 1.4	-18.1 ± 1.1	0.17
Septal	-15.4 ± 2.1	-17.5 ± 1.9	0.09
Lateral	-18.7 ± 2.1	-19.5 ± 1.9	0.49
Peak diastolic circumferential strain rate (%·s^{-1})			
Global	38.1 ± 7.5	38.7 ± 6.8	0.88
Septal	37.0 ± 10.0	40.5 ± 6.3	0.50
Lateral	39.7 ± 6.9	42.7 ± 9.0	0.50
MVO_2 (µl/beat/gram)	1.4 ± 0.2	1.6 ± 0.3	0.18
Total MVO_2 (ml·min^{-1})	0.15 ± 0.02	0.12 ± 0.03	0.12
MEE (%)	49.5 ± 6.1	47.9 ± 7.6	0.70

Data are presented as mean with standard deviation. MAP: mean arterial pressure; LV: left ventricular; SV: stroke volume; MVO_2: myocardial oxygen consumption; MEE: myocardial external efficiency.

Figure S1. MEE/BSAValues corrected by body surface area.

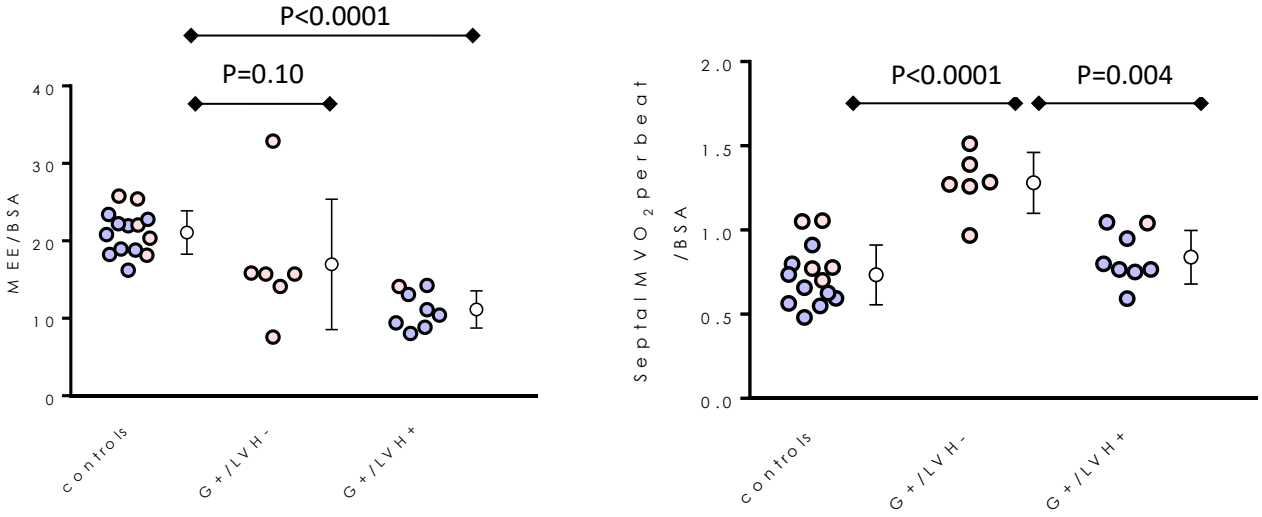

Myocardial external efficiency (MEE; left panel) and septal oxygen consumption (right panel) corrected by body surface area (BSA).